Technology in Cancer Research and Treatment
ISSN 1533-0346
Volume 10, Number 2, April 2011

Diagnostic Potential of Stokes Shift Spectroscopy of Breast and Prostate Tissues – A Preliminary Pilot Study

www.tcrt.org

J. Ebenezar, Ph.D.[1*]
Y. Pu, Ph.D.[2]
C. H. Liu, B.S.[2]
W. B. Wang, Ph.D.[2]
R. R. Alfano, Ph.D.[2]

[1]PG & Research Department of Physics, Jamal Mohamed College (Autonomous), Tiruchirappalli – 620020, Tamilnadu, India
[2]Institue for Ultrafast Spectroscopy and Lasers, Department of Physics, The City College of the City University of New York, 160 Convent Avenue at 138th Street, New York, NY 10031 USA

Stokes Shift (SS) Spectroscopy (SSS) of normal and abnormal breast and prostate tissues were studied. SS spectra is measured by simultaneously scanning both the excitation and emission wavelengths while keeping a fixed wavelength interval of $\Delta\lambda$ = 20 nm. Characteristic, highly resolved peaks and significant spectral differences between normal and different pathological tissues of breast and prostate tissues were observed. The SS spectra of normal and different pathological breast and prostate tissues show the distinct peaks around 300, 350, 450, 500 and 600 nm may be attributed to tryptophan, collagen, NADH, flavin and porphyrin, respectively. Results of the current study demonstrate that the SS spectral changes due to tryptophan, collagen, hemoglobin, NADH, FAD and porphyrin have good diagnostic potential; therefore can be targeted as native tumor markers.

Key words: Stokes shift spectroscopy; Stokes shift; Breast cancer; Prostate cancer; Tissues; Fluorophores; Fluorescence.

Introduction

The objective of the present study is to assess the diagnostic potential Stokes Shift Spectroscopy (SSS) of normal and abnormal breast and prostate tissues. Breast cancer is the second most common malignant tumor among women throughout the world (1) while prostate cancer affects men (1). It was estimated that 207,090 new cases of invasive breast cancer were expected to occur among women and about 39,840 women might die of breast cancer in US during 2010 (1). Early detection of cancer can play a significant role in its treatment, making possible improvement in the quality of the patient's lives and increase in survival rates. If diagnosed early, breast cancer can be treated and cured. The common screening methods for breast cancer detection(s) are physical exam, X-ray mammography, ultrasound, and magnetic resonance imaging (MRI). X-ray mammograms are useful in detecting small tumors that may be unnoticeable by physical exam; however, it uses ionizing radiation and requires uncomfortable breast compression. It also suffers from a significant number of false positives that often lead to unnecessary biopsy. Furthermore, all the three techniques such as X-ray mammography, ultrasound and MRI provide high spatial resolution, but comparatively little information about molecular level changes in breast tissues. While prostate cancer is the second leading cause of cancer death in American men. An estimated 217,730 new prostate cancer cases were expected to occur and among them 32,050 men might die of prostate cancer in US during 2010 (1). Currently, prostate cancer detection is based on digital rectal examination (DRE), prostate specific antigen (PSA) blood test, trans-rectal ultrasound (TRUS) imaging and biopsy. These techniques are not able to detect early stages of cancer. It is well

[*]Corresponding Author:
Jeyasingh Ebenezar, Ph.D.
E-mail: ebey_ebenezar@yahoo.com

known that diagnosis of a small premalignant lesion critical for the success of cancer therapy is a key to increasing survival rates. Consequently, new detection methods are needed for breast and prostate cancers that can overcome current limitation for *in situ* diagnoses and treatment.

Optical spectroscopic techniques examine the interactions of light with biological tissue and they can provide information about the biochemical and structural tissue composition. This method has been called optical Biopsy (OB) noted by Alfano (2). The basic idea behind the operation of OB involves illumination of suspicious lesions with suitable light source and recording the fluorescence spectra emitted by endogenous fluorophores such as tryptophan, collagen, reduced form of nicotinamide adenine dinucleotide (NADH), flavin adenine dinucleotide (FAD) and endogenous porphyrins. The presence of disease results in alteration in the concentration of these fluorophores as well as the light scattering and absorption properties of the tissue, due to changes in blood concentration, nuclear size distribution, collagen content, and epithelial thickness which leads to variation in spectral shape and intensity. However each native fluorophore has a distinct wavelength for absorption and a characteristic wavelength of emission spectrum (3). The fluorescence emission/excitation spectroscopy, emission spectra at one or more excitation wavelengths or excitation spectra corresponding to one or more emission wavelengths have been used for diagnostic purpose (4). A limitation of many clinical studies to date has been the relative paucity of information on the fluorescence excitation and emission wavelengths that optimize the diagnostic sensitivity and/or specificity. OB offers a challenging problem for native fluorescence based techniques, because the optimum condition is probably different for different organs and even for different stages of disease in a given organ. Nevertheless, despite the ability to select both the excitation and emission wavelengths, the conventional laser-induced fluorescence (LIF) spectroscopic method for cancer detection has limited applicability since most fluorescence spectra of complex structures such as tissue result in superimposition of a series of overlapping bands from different fluorophores. It often cannot be resolved satisfactorily by single excitation wavelength. To overcome this problem, multiple excitation technique is used to generate an excitation-emission matrix (EEM) in order to identify the optimal excitation wavelengths at which tissue classification is enhanced and determine the origin of the measured fluorescence signal in a more reliable manner (5). An EEM measurement also requires a series of many fluorescence emission scans at sequential excitation wavelengths at small wavelengths intervals which are time consuming. This is particularly important for those fluorescence instruments that employ single channel optical detectors such as the photomultiplier tube. To speed up spectral acquisition, it is desirable to employ a single excitation wavelength to obtain most of the key fluorophores for tissue characterization in a single scan.

Alternatively, stokes shift spectroscopy (SSS) is a novel rapid method, combining absorption and fluorescence properties of the tissue fluorophores that can be used as a potential tool for the diagnostic purposes. Alfano and Yang were first to introduce the physical concept of SSS and demonstrated the use of SSS of human tissue and key biomolecules (6). In SSS, the excitation wavelength (λ_{ex}) and the emission wavelength (λ_{em}) are scanned synchronously with a constant wavelength interval ($\Delta\lambda = \lambda_{em} - \lambda_{ex}$) between the excitation and emission monochromators throughout the spectrum.

As a result, the intensity of SS signal can be written as:

$$I_{ss} = Kcd\, E_x(\lambda - \Delta\lambda)\, E_m(\lambda)$$

where K is a constant factor accounting for the variation in the molar extinction coefficient with respect to the intensity distribution; c is the concentration of fluorophores; d is the path length of the photons; and E_x and E_m are the intensity distribution patterns of the excitation and emission respectively. For well-defined absorption and quantum yield maximum, the optimum value of the band width $\Delta\lambda$ is set by the difference in wavelength of the emission and excitation maxima which is known as Stokes's shift (SS). As indicated in the above expression, the wavelength of the SS spectra is the combination of both excitation and emission wavelengths and they do not represent either emission or excitation wavelengths individually. The SS spectra can be represented as a diagonal scan of the EEM with a fixed wavelength different between the excitation and emission wavelengths. As the stokes shift spectral intensity involves both the excitation and emission distribution to observe a peak, it is sufficient that either of the two functions $E_x(\lambda - \Delta\lambda)$ or $E_m(\lambda)$ is resolved structure in the measured spectral range. When the wavelength interval $\Delta\lambda$ between λ_{ex} and λ_{em} is chosen properly, the resulting SS spectrum will show features that are more and better resolvable than conventional fluorescence spectrum measured for fixed excitation wavelength. For example, if the wavelength interval is chosen to be the difference between the wavelength of the maximum absorption peak (or excitation peak) and the wavelength of the maximum emission peak for a single fluorophore, the SS spectrum of a sample containing this fluorophore will show a single sharp peak associated with this fluorophore. Therefore, SSS provides a better resolved structure from a composite system, like tissue, in contrast to generally featureless and broadband appearance of the conventional fluorescence spectra.

This technique has been extensively studied for mulitcomponent analysis in analytical chemistry (7) and recently it has been applied for cancer diagnosis (6, 8, 9). However, to the

best of our knowledge, no reports are available on the use of SSS technique in the characterization and spectral discrimination of various pathological stages of breast and prostate tissue from the normal. In this context, the primary objectives of the present pilot study are (i) to introduce SSS in the investigation of normal and different pathological breast and prostate tissues and to explore its capabilities to discriminate between the tissues (ii) optimizing the offset wavelength $\Delta\lambda$ (iii) identifying the highly resolved SS bands using standard fluorophores and (iv) interpretation of SS spectral discrimination between normal and different pathological tissues of breast and prostate tissues using key fluorophores. The contemplated research is intended to significantly increase the use of SSS within a multiplicity of tissues and a variety of diagnostic procedures.

Materials and Methods

Breast Tissues

The SS spectra of normal and different pathological tissues of breast and prostate tissues were studied. A total of 30 fresh human breast tissue samples were obtained from patients undergoing lumpectomy or mastectomy of various pathological conditions of breast tissues were collected from 20 patients, attending the Government Royapettah hospital, Chennai, India. Informed consent of the subjects and institutional review board approval were obtained before the experiment. Of the 30 biopsy samples, 10 paired normal and fibroadenoma samples were collected from the 10 patients with mean age of 27 years (ranges of 22-38 years) and 9 of the 10 patients were premenopausal and only 1 was postmenopausal. (*i.e.*) All the normal samples were collected from approximately 1–2 cm away from uninvolved areas of the region of patients with fibroadenoma site. Remaining 10 infiltrating ductal carcinoma (IDC) samples were collected from 10 patients separately with mean age of 55 years (ranges of 45-57 years) and all the 10 patients were postmenopausal. Immediately after resection the tissue samples were rinsed with 0.9% physiological saline (pH = 7.4) and stored at 4ºC in ice box until SSS study, which took place 2–4 h after resection. At the time of SSS study, a sample was brought to room temperature and moistened with saline.

In another study, a total of 13 fresh human prostate tissue samples were collected from various pathological conditions of prostate disease of 8 patients from National Disease Research Interchange (NDRI) and the Cooperation Human Tissue Network (CHTN). Informed consent of the subjects and institutional review board approval were obtained before the experiment. Of the 13 biopsy samples, 5 paired normal and benign samples were collected from the 5 patients. (*i.e.*) All the normal samples were collected from approximately 1–2 cm away from uninvolved areas of the region of patients with benign site. Remaining 3 malignant prostate tissue samples were collected from 3 patients separately. Immediately after resection the tissue samples were rinsed with 0.9% physiological saline (pH = 7.4) and stored at –20ºC until the SSS study was ready to be performed.

After acquisition of the SSS spectra, the exact site of the all tissue samples were fixed in 10% formalin and sent for histopathologic evaluation performed by an experienced breast and prostate pathologist blinded to the spectroscopy results. The spectroscopic data were classified according to their post-spectroscopy pathology indicates into three groups such as normal, fibroadenoma and IDC for breast tissues and normal, hyperplasia and malignant for prostate tissues.

SS Spectral Measurements

SS spectral data acquisition of breast and prostate tissues was measured by different commercial spectrofluorometer system of their schematic instrumentation is shown Figure 1. Both

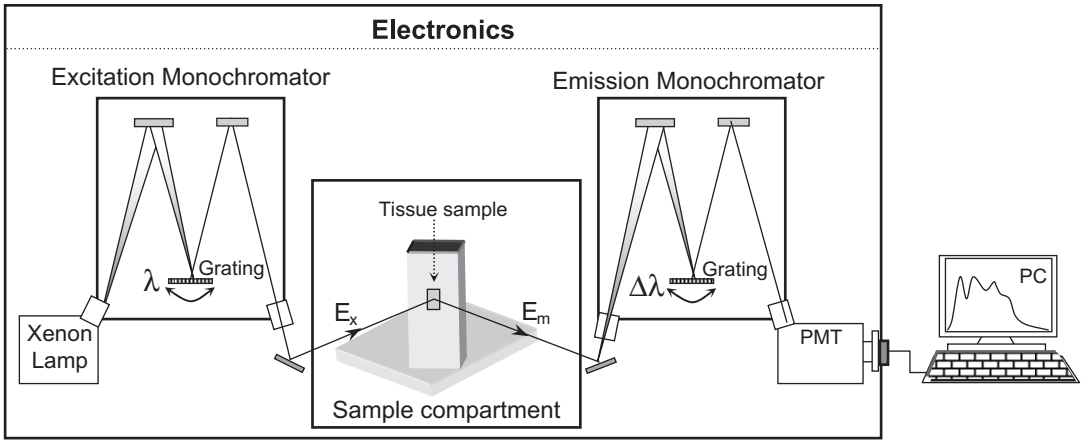

Figure 1: Schematic of the experimental instrumentation for SSS *in vitro* study. The arrows in the excitation and emission monochromator represent the direction of rotation of the grating and Ex and E_m represent the direction of excitation and emission light.

instrument consists of a 150 W xenon lamp is a light source, an excitation monochromator, a sample compartment and an emission monochrmator equipped with a photomultipler tube detector (PMT). A personal computer (PC) controlled spectral data acquisition.

SS spectra of *ex vivo* breast tissues were recorded using spectrofluorometer (Fluoromax-2, ISA, Jobin Yvon-Spex, New Jersey, USA). The biopsy samples size about 5 × 5 × 2 mm^3 or smaller were mounted in a block between the bracket and spring clip and placed in a sample holder compartment for front face emission sample accessory. Light from xenon lamp of pre-selected wavelength, with a size of approximately 2 mm x 4 mm was allowed to fall on the tissue sample and the emitted light was collected at approximately 22.5º angle to the excitation light. The excitation and emission monochromators having fixed band passes of 3 nm each and the integration time and wavelength increment were set at 0.1 s and 1.0 nm, respectively. The collected signal is transferred to a PC.

While SS spectra of *ex vivo* prostate tissues were recorded using spectrofluorometer (LS 50, Perkin Elmer, Shelton, Connecticut, USA). Defrosted prostate tissue biopsies were solid chunks of size 5 × 5 × 2 mm^3 are smaller were placed moist in a quartz cuvette with the epithelium towards face of the cuvette and the beam. The excitation light of size approximately 2 mm × 4 mm was incident perpendicular to the face of the tissue epithelium surface and the emitted fluorescence light was collected at 90º angle to the excitation light for right angle emission sample accessory. During the data acquisition of prostate tissue measurement, the excitation and emission monochromators having fixed band passes of 6 nm each and the wavelength increment were set at 0.5 nm. The variation in the excitation light source intensity as a function of wavelength was accounted during SS spectra measurements. This was done by detecting the fluorescence signal (S) by the PMT as well as recording the reference excitation intensity (R) by a photodiode and taking their ratio S/R to serve as the final SS signal to account for the wavelength-dependent light intensity.

Optimization of Offset Wavelength Δλ

The SS is dependent on the polarity of the host environment surrounding the emitting organic molecule but of most interest, the width of the SS spectrum can be simply compressed or expanded just by decreasing or increasing the Δλ parameter (6). The decrease of SS signal is advantageous since the spectral overlap greatly reduces. During SS spectral acquisition, the excitation and emission monochromator were scanned simultaneously at the same speed with constant wavelength interval (Δλ) between them. In our study, we tried various Δλ values ranging from 10 nm to 50 nm insteps of 10 nm. Among all the Δλ values, Δλ = 20 nm showed an identifiable key fluorophores with good SNR and hence the value of Δλ = 20 nm was set as the optimal offset wavelength for the entire experiment with scan speed of 5 nm/sec. The SS spectra of normal, fibroadenoma and IDC breast tissues were recorded in the wavelength region 250 to 750 nm at Δλ = 20 nm. The SS spectra of normal, hyperplasia and malignant prostrate tissues were recorded in the wavelength region 250 to 600 nm at Δλ = 20 nm.

Results

The averaged SS spectra of normal, fibroadenoma and IDC breast tissues in the wavelength region between 250 nm and 750 nm are shown in Figure 2. The normal tissues showed three primary peaks observed at 303, 350 and 510 nm. Fibroadenoma tissues exhibit single primary peak found at 350 nm showing higher fluorescence intensity than other bands. IDC tissues showed bands similar to those of normal and fibroadenoma tissues but it has lower fluorescence intensity.

The normalized averaged SS spectra of normal, fibroadenoma and IDC breast tissues in the wavelength region between 250 nm and 750 nm are shown in Figure 3. From this spectrum, it is observed that normal tissues showed peaks at 303, 350, 450, 510 and small hump found around 595 and 650 nm. Fibroadenoma tissues revealed similar spectral signature with primary fluorescence emission peak found at 350 nm showing higher fluorescence intensity compared to normal and IDC tissues. At longer wavelengths, fibroadenoma tissues showed lower fluorescence intensity than normal and IDC tissues. However, it is interesting to note that the characteristic SS spectral signatures of IDC tissues show an entirely different pattern with distinct well resolved emission band at 493, 598, 622 and 648 nm predominating over other bands observed at 300, 350 and 450 nm which shows lesser intensity compared to normal and fibroadenoma tissues. In addition to that a spectral valley observed around 405 nm for normal, fibroadenoma and IDC breast tissues respectively.

The averaged SS spectra of normal, hyperplasia and malignant prostate tissues in the wavelength region between 250 nm and 600 nm are shown in Figure 4. The normal tissues show single primary band around 345 nm and a secondary peaks observed around 307, 440 and 510 nm. Whereas hyperplasia tissues exhibit two primary bands around 297 and 345 nm with higher fluorescence intensity than normal tissues. However, malignant prostate tissues revealed similar spectral signature with lesser fluorescence intensity compared with hyperplasia tissues.

The normalized averaged SS spectra of normal, hyperplasia and malignant prostate tissues in the wavelength region between 250 nm and 600 nm are shown in Figure 5. From this spectrum, it is observed that normal tissues show small hump around 307 nm and primary prominent peak centred at

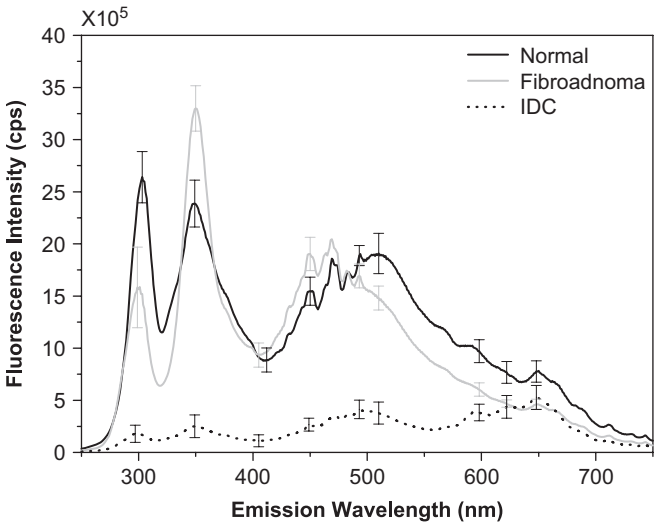

Figure 2: Averaged SS spectra of normal, fibroadenoma and IDC breast tissues.

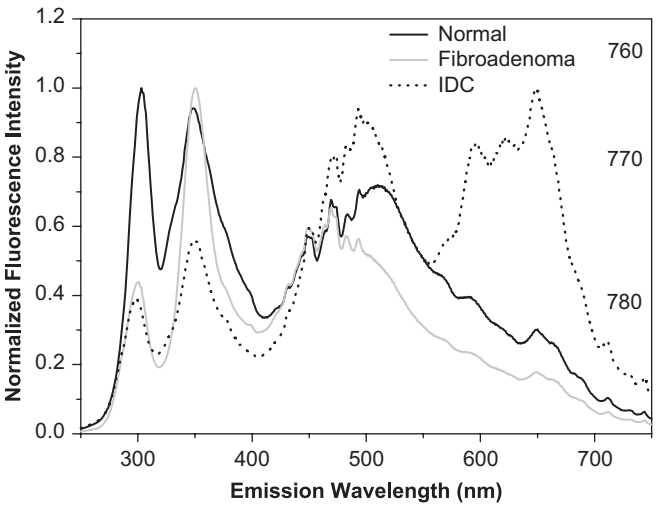

Figure 3: Normalized averaged SS spectra of normal, fibroadenoma and IDC breast tissues.

345 nm with secondary peaks was observed at 440 and 510 nm. The hyperplasia and malignant tissues exhibit two primary highly resolved peaks at 297 and 345 nm with secondary peaks was observed at 440 and 510 nm. It is to be noted that, primary fluorescence band observed at 297 and 299 nm for hyperplasia and malignant tissues showing higher fluorescence intensity than normal tissues. However, normal tissues showing higher fluorescence intensity at 350 nm compared with hyperplasia and malignant tissues.

SS Spectral Measurements of Standard Fluorophores

In order to confirm the origin of the observed spectral peaks from breast and prostate tissues and assign them to various native fluorophores, the SS spectra of commercially grade fluorophores (Sigma Chemicals, USA) such as tryptophan, collagen, NADH, FAD were measured in their powder form with same experimental parameters maintained as for the breast tissues. But porphyrin fluorophore dissolved in a methanol was made into a solution form and their SS spectra were measured from the quartz cuvette.

Figure 6 shows the normalized SS spectra of the standard fluorophores such as tryptophan, collagen, NADH, FAD and porphyrin of their narrow emission peaks observed at 311, 353, 397, 533, and 601 respectively. Another interesting feature was noted that, porphyrin showing secondary peaks at 622 and 650 nm respectively. Further, the fine structures observed in the wavelength region between 440 and 500 nm may due to the stray light contribution from the xenon lamp

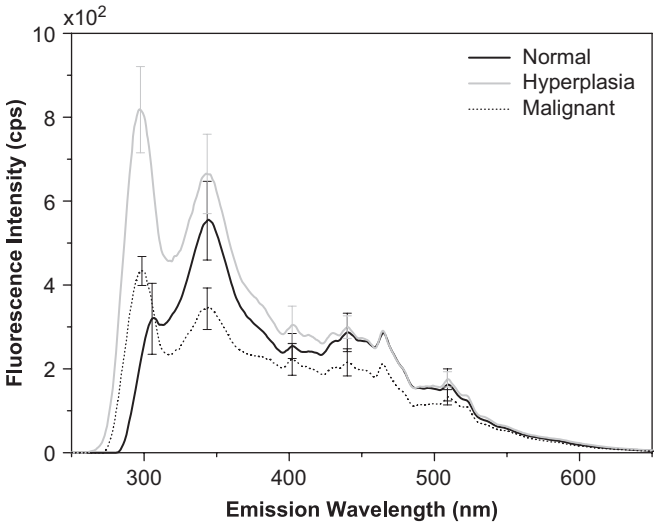

Figure 4: Averaged SS spectra of normal, hyperplasia and malignant prostate tissues.

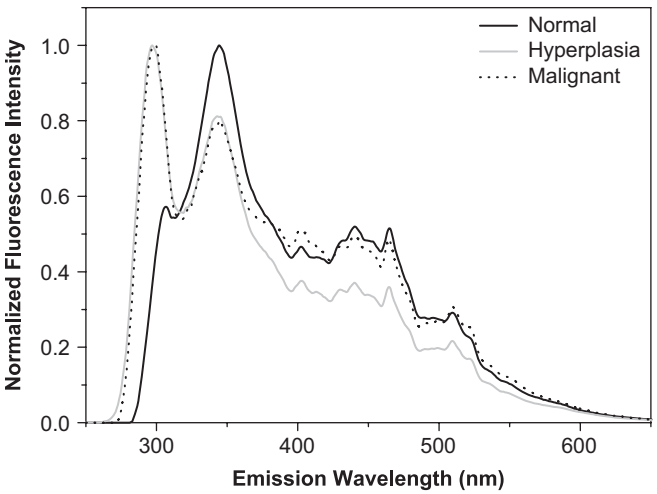

Figure 5: Normalized SS spectra of normal, hyperplasia and malignant prostate tissues.

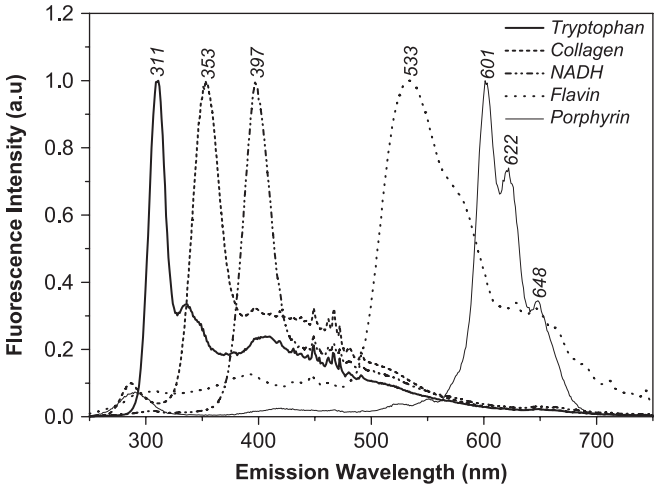

Figure 6: Normalized SS spectra of standard fluorophores of tryptophan, collagen, NADH, FAD and Porphyrin.

passing through the exit slit of the excitation monochromator with sharp spectral features were observed at 467 nm due to the contribution from the xenon lamp source.

Discussion

The diagnostic potential of SSS technique for spectral characterization of normal and abnormal breast and prostate tissues is demonstrated. The origin of the observed spectral peaks around 300, 350, 450, 490, 510 and 600 nm from normal and abnormal breast and prostate tissues was identified and assigned them to various native fluorophores such as tryptophan, collagen, NADH, FAD and porphyrin respectively. We thus tentatively, identify these biochemical compounds as major endogenous fluorophores of breast and prostate tissues. In addition to that, the sharp spectral features are observed at 467 nm due to the contribution from the xenon lamp source.

Distinct differences in the spectral signatures of tryptophan, collagen, hemoglobin, NADH, FAD and porphyrin were observed from normal and different pathological conditions of breast tissues. As it had been noted earlier, normal tissues exhibits two prominent peaks observed around 303 and 350 nm. The peak observed at 303 nm most likely due to tryptophan which is significantly weaker for fibroadenoma and IDC tissues. Further, the peak emission wavelength was blue shifted to 299 and 297 nm fibroadenoma and IDC tissues with respect to normal tissues. The considerable differences in the relative fluorescence intensity and the peak position wavelength of tryptophan emission between normal and different pathological conditions of breast tissues may be attributed to the changes in the microenvironment and conformational conditions of the protein bound tryptophan, relative to the free amino acid (10).

The second prominent peak was observed in the normal tissues at 350 nm corresponding to structural protein collagen which is drastically decreases in the cases of IDC tissues may be due to matrix metalloproteinases released from epithelial cells and this may cause degradation of collagen cross-links, are usually present in tissue areas undergoing significant architectural changes during neoplastic transformation. Volynskaya *et al* found that there was decreased collagen fluorescence in malignant breast tissues due to fragmentation and disorganization of the collagen fibers in the stroma of invasive cancers due to action matrix metalloproteinases (11). In addition to that, the observed fluorescence intensity decrease could be attributed to thickening of the epithelium, which results in less excitation light reaching the underlying collagen network (5). But it is to be noted that, the fibroadenoma tissues showed higher collagen fluorescence intensity due to less fatty tissues which are characterized by higher amount of collagen than normal and IDC tissues (11). Earlier reported studies shown that the normal breast tissue fluorescence contribution of the collagen content decreased with increasing adipose tissue content, while it increased with increasing fibro-connective tissue content (12). This agrees with the fact that the relative amount of collagen fluorescence is higher in fibroadenoma tissues that become densely fibrotic of the breast as the patient age (13). Similar observations were also reported by Taroni *et al* measured absorption of collagen in normal breast tissues using time-resolved transmission spectroscopy for breast tissue characterization and showed that less fatty tissues are characterized by higher collagen concentration (14). Thus the above factors may explain the reason for significantly higher collagen fluorescence in fibroadenoma tissues, as compared with normal and IDC tissues tissues.

The characteristic hemoglobin absorption features were clearly found as a dip at 410, 408, and 405 nm for normal, fibroadenoma and IDC tissues respectively. The hemoglobin absorption is deeper in the case of IDC tissues than normal and fibroadenoma tissues due to possible increase in hemoglobin content because of angiogenesis (3, 11). As most malignant tumors including IDC tissues had a higher blood volume that are characterized by increased vasculature (angiogenesis) compared to nonmalignant tissues, which is also consistent with the findings of earlier studies reported by Demos *et al* (3), Volynskaya *et al* (11) and Zhu *et al* (12).

The sharp spectral peak at 450 nm of the normal tissue may be due to coenzyme of NADH, which are slightly increases for fibroadenoma and IDC tissues. This change due to an increased number of cells and/or increased level of metabolic activity in epithelial cells and the relative concentration of

this fluorophore vary according to the oxidative metabolic status of the cells (11, 12, 15). This observation is in agreement with reported studies which have shown that the fluorescence of adipose tissues would be expected to have less contribution from NADH than that benign and IDC breast tissues (11, 12).

The normal tissues exhibit prominent primary peak at 493 nm followed by broad band centered around 510 nm. Whereas in the case of fibroadenoma tissues are revealed similar spectral signature with lesser fluorescence intensity compared to normal tissues. Further, it is interesting to note that the IDC tissues exhibits characteristic well pronounced emission peak was observed at 493 nm with increased broad band was observed around 510 nm compared to that normal and fibroadenoma tissues. The spectral peaks observed around 493 and 510 nm may be attributed to emission of FAD. Results of our study also showed that there is a substantial increase of FAD fluorescence from IDC tissues due to rapidly multiplying neoplastic cells and/or influenced by oxidation tissue fluorophore leading to increased amount of FAD fluorescence compared with normal and fibroadenoma breast tissues (2, 16).

Another spectral feature was found at longer wavelength from IDC tissues; we noticed three highly resolved peaks were observed around 600, 622 and 650 nm. The peak at 650 nm is highly resolved as compared with other peaks. It is interesting to note that these peaks were absent in case of normal and fibroadenoma breast tissues rather a two small hump with lesser intensity was observed around 595 and 650 nm. The fibroadenoma tissue shows lower intensity emission in the wavelength region 550 to 750 nm as compared to normal and IDC tissues. Results of our study suggest that, the observed highly resolved peaks from IDC tissues around 600, 622 and 650 nm indicating that high amounts of endogenous porphyrins that are known to accumulate in the neoplastic tissues (2).

Distinct salient differences in the spectral signatures of tryptophan, collagen, NADH, and FAD were observed from normal and different pathological conditions of prostate tissues from Figure 4. The normal tissues exhibit small peak around 307 nm most likely due to tryptophan which was significantly higher for hyperplasia and malignant tissues. This increase is probably due to hyperactivity or epithelium glandular proliferation resulting in higher transient concentration of proteins in cells and/or increased thickness of the epithelium (5). In addition to the increase in tryptophan fluorescence intensity, the peak emission wavelength was blue shifted to 297 and 299 nm for hyperplasia and malignant tissues with respect to normal tissues. The considerable differences in the relative fluorescence intensity and the peak position wavelength of tryptophan emission between normal and different pathological conditions of prostate tissues may be attributed to the changes in the microenvironment and conformational conditions of the protein bound tryptophan, relative to the free amino acid (10). Based on the results observed from the present study, it is suggested that changes in intrinsic tryptophan fluorescence and their peak emission wavelength from hyperplasia and malignant prostate tissues can be used as one of the diagnostic criteria to classify the early neoplastic changes.

The primary prominent peak was observed in the normal tissues at 345 nm corresponding to structural protein collagen which is drastically decreased in the cases of hyperplasia and malignant prostate tissues. The spectral changes produced by structural and biochemical changes in the epithelium and subepithelial collagen network may be due to crowded epithelial cells with increased variability in shape and size and overall thickening of the epithelium (5, 17). Thus, increased thickness of the epithelium in hyperplasia and malignant prostate glands attenuates both excitation light and emission fluorescence light from the collagen network, leading to reduced penetration depth of the excitation light as well as the reabosrption of the emitted fluorescence.

Although changes in the tryptophan, collagen contribution to the overall SS spectra differentiate normal from abnormal tissues, a substantial difference in the NADH and FAD contribution is found in abnormal when compared with normal prostate tissues. The normal tissue shows a broad peak in the wavelength region 425 to 450 nm with sharp spectral peak is found at 440 nm may be due to the coenzyme NADH, which is decreased intensity for hyperplasia and malignant tissues. This decrease of NADH fluorescence in early stages of tissue transformation such as hyperplasia and malignant tissues may be due to changes in tissue morphology in particularly thickening of epithelium and oxidative metabolic status of the tissues (5, 11). At longer wavelength region, normal tissues exhibit prominent peak at 510 nm. In the case of hyperplasia tissues are revealed similar spectral signature with lesser fluorescence intensity compared to normal tissues. Malignant tissues show slightly increasing intensity at 510 nm compared to normal and hyperplasia tissues. There is a substantial increase in FAD fluorescence from malignant tissues indicates that number of neoplastic cells and oxidative metabolic activity associated with progression of neoplastic disease leads to increased amount of FAD fluorescence compared normal and hyperplasia tissues (2, 16).

The present result of the overall SS spectral profile of breast and prostate tissues provides information not only about their tissue architecture (epithelial thickness) and organization but also about their metabolic state and concentrations of fluorescing molecules, which can be correlated to histological changes. The alterations in tissue architecture and cellular composition induced by process such as hyperplasia, dysplasia and invasive carcinoma are reflected in variations in the

optical properties of human tissues. Thus, alterations in tissue architecture that inhibit the ability of excitation photons to reach the native fluorophores or of the fluorescence emission photon to escape from the tissue could be detected by the spectroscopic system would affect the fluorescent signature. Additionally, changes in the concentration of natural fluorophores could alter the emitted fluorescence in a single scan which is presented in our study. By measuring the SS signal from normal and different pathological conditions of breast and prostate tissues information concerning a disease condition can be obtained.

SSS technique has an added advantage for that all the key native active fluorophores in tissue are excited under optimal conditions such as wavelength of excitation, slit widths, scan speed, and scan range which are practically impossible in the case of conventional fluorescence measurements. In the case of conventional fluorescence measurements, optimal conditions are chosen based on the fluorophores of interest. Though, EEM offers greater resolution, it is time consuming to carry out even with multi-channel detectors. Also, the large amount of data of EEM could significantly slow down the data processing procedures. On the other hand, SSS spectrum represents the faster diagonal scan over the entire EEM, thereby reducing the time of data acquisition without any alterations in the details over the entire spectral range of the different fluorophores present in the tissues. Further, in EEM, emission bands of different fluorophores are obtained for different excitation wavelengths, whereas SSS which needs a suitable single excitation ($\Delta\lambda$) wavelength, is sufficient to obtain most of the tissue fluorophores in a single scan. Further, it can be implemented in real time during surgery. In addition to these SSS technique has several features such as (i) SSS can effectively examine the different fluorophores in tissues by choosing appropriate $\Delta\lambda$ in a single scan itself which results in reduction of time required for data acquisition. (ii) The SSS technique reduces overlapping interferences between the multiple fluorophores and also reduces the bandwidth of each of the fluorescence peak of individual fluorophores. (iii) The possibility of each fluorophore can be identified in a specific spectral range with highly resolved spectral bands.

These features greatly simplify the qualitative interpretation of SS spectra between normal and different pathological breast and prostate tissues. In order to improve the diagnostic capability of optical spectroscopy for breast and prostate cancer diagnosis, SSS is a novel technique one can analyze key biochemical markers such as tryptophan, collagen, hemoglobin, NADH, FAD and porphyrin that can now be obtained in single scan (6); and hence they can be targeted as a tumor markers for normal and different pathological stages of the breast and prostate. On the basis of above factors, SSS may also be considered as an alternative or/and a complementary technique with the existing conventional methods for tissue diagnosis. One limitation of the SSS that was observed during front face emission geometry is that the SS measurements involved the simultaneous scanning of both excitation and emission monochromators, significant contribution from the excitation light source was expected. As a result sharp peaks (strong scattering background signal) were found to arise in the wavelength range 440-500 nm. These may attributed to the small contribution of the stray light from the xenon lamp, penetrating through the excitation monochromator. This penetration could not be eliminated here since for small $\Delta\lambda$ values. This is because of the fact that, the spectrofluorometer used in this study was equipped with single excitation and single emission monochromators only. The rejection ratio of the excitation monochromators for light outside the passing band is finite, and the stray light from the xenon lamp whose spectrum overlaps with fluorescence from the tissue fluorophore could produce strong scattering background that lead to dominance of the fluorescence spectra of wavelength range 440-500 nm (9). To overcome this, we divided each SS tissue spectra by the lamp spectra measured under the same instrumental parameters minimized the contribution from the excitation light source to the SS tissue spectra in this study. However we feel that, the best solution could be to use a spectrofluorometer equipped with double excitation and emission monochromator since it has high stray light rejection ratio. As a result this stray light is prevented not only from interfering with the fluorescence signal, but also at the same time, prevented from entering into the emission monochromator.

In conclusion, this limited pilot study suggests that SSS has a potential method to differentiate diseased from normal breast and prostate tissues *in vitro* which should be used *in vivo*. Results of the current study demonstrate that spectral changes due to tryptophan, collagen, NADH, FAD and porphyrin have good diagnostic potential. As a preliminary investigation, we have studied a several cases in each diseased group. In this regard, more detailed investigations on a large population consisting of different pathological precancerous breast and prostate tissues would be necessary. Furthermore, such investigations with a large group of tissue biopsies will also be useful for the development of a statistical evaluation that could facilitate for real time *in vivo* clinical diagnosis of breast and prostate cancer and can be extended to the cervix, colon and lung.

Acknowledgments

The author J.E. wishes to thank Dr. S. Ganesan and Dr. P Aruna at Division of Medical Physics & Laser, Anna University, Chennai. The author E.J. also thanks Dr. Senekalatha, surgical oncologist, Department of Oncology, Government of Royapettah Hospital, Chennai for providing the breast tissues used in this study. This research is supported in part

by U. S. Army Medical Research and Material Command under grant of # W81XWH-08-1-0717 (CUNY RF 47170-00-01). The authors acknowledge the help of CHTN for providing normal and abnormal prostate tissue samples for the measurements.

References

1. Cancer facts and Figures. Atlanta (GA): *American Cancer Society* (2010).
2. Alfano, R. R., Tata, D. B., Cordero, J., Tomashefsky, V., Longo, F. W., Alfano, M. A. Laser induced fluorescence spectroscopy from native cancerous and normal tissues. *IEEE J Quantum Electron 20*, 1507-1511 (1984).
3. Demos, S. G., Vogel, A. J., Gandjbakhche, A. H. Advances in optical spectroscopy and imaging of breast lesions. *J Mammary Gland Biol Neoplasia 11*, 165-181 (2006).
4. Yang, Y., Celmer, E. J., Szczepaniak, M. Z., Alfano, R. R. Excitation spectrum of malignant and benign breast tissues: A potential optical biopsy approach. *Lasers Life Sci 7*, 249-265 (1996).
5. Zheng, W., Lau, W., Christopher, C., Soo, K. C., Oliva, M. Optimal excitation-emission wavelengths for autofluorescence diagnosis of bladder tumors. *Int J Cancer 104*, 477-481 (2003).
6. Alfano, R. R., Yang, Y. Stokes shift emission spectroscopy of human tissue and key biomolecules. *IEEE Quantum Electron 9,* 148-153 (2003).
7. T. Vo-Dinh. Multicomponent analysis by synchronous luminescence luminescence spectrometry. *Anal Chem 50*, 396-401 (1978).
8. Ebenezar, J., Aruna, P., Ganesan, S. Synchronous fluorescence spectroscopy for the detection and characterization of cervical cancers | in vitro. *Photochem Photobiol* 86, 77-86 (2010).
9. Liu, Q., Grant, G., Vo-Dinh, T. Investigation of synchronous fluorescence method in multicomponent analysis in tissue. *IEEE J Quantum Electron 16*, 4, 927-940 (2010).
10. Lackowicz, J. R. *Principles of fluorescence Spectroscopy.* (second edition) Plenum Press, New York (1999).
11. Volynskaya, Z., Haka, A. S., Bechtel, K. L., Fitzmaurice, M., Shenk, R., Wang, N., Nazemi, J., Dasari, R. R., Feld, M. S. Diagnosing breast cancer using diffuse reflectance spectroscopy and intrinsic fluorescence spectroscopy. *J Biomed Opt* 13, 024012 (2008).
12. Zhu, C., Palmer, G. M., Breslin, T. M., Harter, J., Ramanujam, N. Diagnosis of breast cancer using fluorescence and diffuse reflectance spectroscopy: a Monte-Carlo-model-based approach. *J Biomed Opt* 13, 034015 (2008).
13. Thomsen, S., Tatman, D. Physiological and pathological factors of human breast disease that can influence optical diagnosis. *Ann NY Acad Sci 838*, 171-193 (1998).
14. Taroni, P., Comelli, D., Pifferi, A., Torricelli, A., Cubeddu, R. Absorption of collagen: effects on the estimate of breast composition and related diagnostic implications. *J Biomed Opt 12*, 014021 (2007).
15. Georgakoudi, I., Jacobson, B. C., Muller, M. G., Sheets, E. E., Badizadegan K., Carr-Locke, D. L., Crum, C. P., Boone, C. W., Dasari, R. R., Van dam, J., Feld, M. S. NAD(P)H and collagen as in vivo quantitative fluorescent biomarkers of epithelial precancerous changes. *Cancer Research 62*, 682-687, (2002).
16. Chance, B., Schoener, B., Oshino, R., Itshak, F., Nakase, Y. Oxidation-reduction ratio studies of mitochondria in freeze-trapped samples. NADH and flavoprotein fluorescence signals. *J Biol Chem 254*, 4764-4771 (1971).
17. Mattthew, M. Prostate gland. *Toronto health and Nutrition* (2008) http://www.atozhealthguide.com/index2.php?optioncom_content&do_pdf=1&id=56-

Received: October 6, 2010; Revised: February 11, 2011; Accepted: February 16, 2011